NAVAL POSTGRADUATE SCHOOL

MONTEREY, CALIFORNIA

THESIS

TIDAL WAVE REFLECTANCE, EVOLUTION AND DISTORTION IN ELKHORN SLOUGH, CA

by

Casey J. Gon

March 2013

Thesis Advisor: James MacMahan
Second Reader: Edward Thornton

Approved for public release; distribution is unlimited

THIS PAGE INTENTIONALLY LEFT BLANK

REPORT DOCUMENTATION PAGE			Form Approved OMB No. 0704–0188
Public reporting burden for this collection of information is estimated to average 1 hour per response, including the time for reviewing instruction, searching existing data sources, gathering and maintaining the data needed, and completing and reviewing the collection of information. Send comments regarding this burden estimate or any other aspect of this collection of information, including suggestions for reducing this burden, to Washington headquarters Services, Directorate for Information Operations and Reports, 1215 Jefferson Davis Highway, Suite 1204, Arlington, VA 22202–4302, and to the Office of Management and Budget, Paperwork Reduction Project (0704–0188) Washington DC 20503.			
1. AGENCY USE ONLY ***(Leave blank)***	**2. REPORT DATE** March 2013	**3. REPORT TYPE AND DATES COVERED** Master's Thesis	
4. TITLE AND SUBTITLE TIDAL WAVE REFLECTANCE, EVOLUTION AND DISTORTION IN ELKHORN SLOUGH, CA		**5. FUNDING NUMBERS**	
6. AUTHOR(S) Casey J. Gon			
7. PERFORMING ORGANIZATION NAME(S) AND ADDRESS(ES) Naval Postgraduate School Monterey, CA 93943–5000		**8. PERFORMING ORGANIZATION REPORT NUMBER**	
9. SPONSORING /MONITORING AGENCY NAME(S) AND ADDRESS(ES) N/A		**10. SPONSORING/MONITORING AGENCY REPORT NUMBER**	
11. SUPPLEMENTARY NOTES The views expressed in this thesis are those of the author and do not reflect the official policy or position of the Department of Defense or the U.S. Government. IRB Protocol number ____N/A____.			
12a. DISTRIBUTION / AVAILABILITY STATEMENT Approved for public release; distribution is unlimited		**12b. DISTRIBUTION CODE**	

13. ABSTRACT (maximum 200 words)

The shoreward and seaward propagating tidal wave components were determined using four co-located pressure and velocity sensors longitudinally deployed in Elkhorn Slough, Monterey Bay, CA, to describe tidal wave evolution and distortion. Elkhorn Slough is short, reflective (~100%) estuary consisting of a narrow, gently sloping main channel and vast marsh and mud flats near the landward boundary. The amplitude reflection for the astronomical tidal constituent is ~90%, whereas the distortion, described by summing all non-astronomical tidal amplitudes, reflection is large (>125%) for all stations stating that the seaward tidal wave is more distorted than the shoreward tidal wave. It was found that the reflective time, defined as the time it takes the tidal wave to propagate to the landward boundary and back, varies as function of tidal elevation. Surprisingly, the reflective time increases with increasing tidal elevation contrary to the hypothesis that the shallow-water tidal wave phase speed increases with increasing tidal elevation, resulting in a reduced time. The landward end of the slough has vast low-lying marshes and mud flats that are inundated during higher tidal elevations, causing the effective (average) wave depth to decrease with increasing tide elevation, which explains why the tidal wave phase speed decreases instead of increasing. The elevation-dependent reflective time caused by a time-varying wave phase speed modifies the shape of the seaward tidal wave relative to the shape of the shoreward tidal wave, which explains the evolution and distortion of a tidal wave in a reflective slough.

14. SUBJECT TERMS tidal, distortion, evolution, reflection, marsh, wave phase speed, Elkhorn Slough			**15. NUMBER OF PAGES** 41
			16. PRICE CODE
17. SECURITY CLASSIFICATION OF REPORT Unclassified	**18. SECURITY CLASSIFICATION OF THIS PAGE** Unclassified	**19. SECURITY CLASSIFICATION OF ABSTRACT** Unclassified	**20. LIMITATION OF ABSTRACT** UU

NSN 7540–01–280–5500 Standard Form 298 (Rev. 2–89)
Prescribed by ANSI Std. 239–18

THIS PAGE INTENTIONALLY LEFT BLANK

Approved for public release; distribution is unlimited

TIDAL WAVE REFLECTANCE, EVOLUTION AND DISTORTION IN ELKHORN SLOUGH, CA

Casey J. Gon
Lieutenant Commander, United States Navy
B.S., United States Naval Academy, 2003
M.B.A., Salve Regina University, 2009

Submitted in partial fulfillment of the
requirements for the degree of

MASTER OF SCIENCE IN METEOROLOGY AND PHYSICAL OCEANOGRAPHY

from the

NAVAL POSTGRADUATE SCHOOL
March 2013

Author: Casey J. Gon

Approved by: Jamie MacMahan
Thesis Advisor

Ed Thornton
Second Reader

Peter Chu
Chair, Department of Oceanography

THIS PAGE INTENTIONALLY LEFT BLANK

ABSTRACT

The shoreward and seaward propagating tidal wave components were determined using four co-located pressure and velocity sensors longitudinally deployed in Elkhorn Slough, Monterey Bay, CA, to describe tidal wave evolution and distortion. Elkhorn Slough is short, reflective (~100%) estuary consisting of a narrow, gently sloping main channel and vast marsh and mud flats near the landward boundary. The amplitude reflection for the astronomical tidal constituent is ~90%, whereas the distortion, described by summing all non-astronomical tidal amplitudes, reflection is large (>125%) for all stations stating that the seaward tidal wave is more distorted than the shoreward tidal wave. It was found that the reflective time, defined as the time it takes the tidal wave to propagate to the landward boundary and back, varies as function of tidal elevation. Surprisingly, the reflective time increases with increasing tidal elevation contrary to the hypothesis that the shallow-water tidal wave phase speed increases with increasing tidal elevation, resulting in a reduced time. The landward end of the slough has vast low-lying marshes and mud flats that are inundated during higher tidal elevations, causing the effective (average) wave depth to decrease with increasing tide elevation, which explains why the tidal wave phase speed decreases instead of increasing. The elevation-dependent reflective time caused by a time-varying wave phase speed modifies the shape of the seaward tidal wave relative to the shape of the shoreward tidal wave, which explains the evolution and distortion of a tidal wave in a reflective slough.

THIS PAGE INTENTIONALLY LEFT BLANK

TABLE OF CONTENTS

THIS PAGE INTENTIONALLY LEFT BLANK

LIST OF FIGURES

THIS PAGE INTENTIONALLY LEFT BLANK

LIST OF TABLES

THIS PAGE INTENTIONALLY LEFT BLANK

LIST OF ACRONYMS AND ABBREVIATIONS

A_c	Cross Sectional Area
ADCP	Acoustic Doppler Current Profiler
A_{hfm}	High Frequency Motion Amplitude Coefficient
A_{lfm}	Low-Frequency Motion Amplitude Coefficient
A_p	Bulk Amplitude from Pressure
A_{pu}	Bulk Amplitude from Pressure and velocity
A_{tot}	Total Amplitude Coefficient
A_u	Amplitude of the High Frequency Motions from Streamwise
b	Channel Width
CA	California
C_g	Shallow Water Wave Group Speed
CSUMB	California State University of Monterey Bay
ES	Elkhorn Slough
η	Sea Surface Elevation
f	Frequency
g	Gravitational Acceleration Constant
h	Depth
h_{avg}	Average Depth
HHW	Higher High Water
HW1	Highway 1
J_o	Bessel Function
K1	Lunar Diurnal Tidal Constituent
L	Tidal Wavelength
LLW	Lower Low Water
M	meters
M2	Lunar Semi-Diurnal Tidal Constituent
M4	Shallow Water Overtide of the Lunar Semi-Diurnal Tidal Constituent
MHz	Megahertz

MB	Monterey Bay
MBSFML	Monterey Bay Sea Floor Mapping Laboratory
NPS	Naval Postgraduate School
O1	Lunisolar diurnal Tidal Constituent
ONR	Office of Naval Research
p	Pressure
R_{hfm}	High-Frequency Motion Tidal Reflection Coefficient
RIVET	River and Inlet Dynamics Experiment
R_{lfm}	Low-Frequency Motion Tidal Reflection Coefficient
ρ	Density of Sea Water
R_{tot}	Total Tidal Reflection Coefficient
s	seconds
σ	Radian Tidal Frequency
ST1	Station 1
ST2	Station 2
ST3	Station 3
ST4	Station 4
u	Streamwise Velocity
v	Cross-Channel Velocity

ACKNOWLEDGMENTS

I would like to express my sincere gratitude to my advisor, Dr. Jamie MacMahan, for his guidance, instruction, and encouragement throughout the course of this research. His dedication, wealth of knowledge, and enthusiasm for science, has made the thesis process both exciting and educational. Thanks for not only being a great advisor but a most trusted friend. I wish you nothing but the best in all of your life's endeavors. I would like to offer my sincere gratitude to my second reader, Dr. Ed Thornton, for his support, encouragement, and expertise. Thank you both.

Words do not even do justice for Jenna Brown's contribution to my thesis. Finishing my thesis would not have been possible without you. Your patience and ability to push me through MATLAB literally saved my sanity. Your sense of humor and outlook on life kept me grounded through the difficult stretches during my time at NPS. I am honored to be considered your friend. Thank you from the bottom of my heart.

I would like to thank Paul Jessen, Mike Cook, Marla Stone, and Keith Wyckoff for your support with all things Science, NPS and MATLAB. The four of you are not recognized nearly enough for everything you do day in and day out to keep this department going and making sure Science happens.

It is also important to acknowledge the other professors at NPS who have inspired so many of us to achieve this milestone in our lives. They have made this an experience I will always remember. Thank you.

To the Naval Postgraduate School's Spring Class of 2013, we made it! To Steve Mcintyre, Erin Ceschini, Angela Lefler, Kate Longley, Paul Kutia, Emre Gulher, and Eric Daley, my endearing thanks.

I want to thank my wife, Pam Gon, for her love and devotion throughout my time at NPS. Her understanding and support have enabled this thesis. I am so blessed to have you in my life.

Finally, I would like to thank my parents, John and Peggy Gon. They have always been my greatest supporters, always believed in me, and are always ready to express their love for me. I dedicate this thesis to you.

THIS PAGE INTENTIONALLY LEFT BLANK

I. MOTIVATION

As the focus of U.S. Navy operations has shifted from the blue water to the brown water to meet the changing threats, it is important that the war fighter has a vast understanding of the physical processes associated with all environments to obtain a competitive advantage against the adversary. To gain a greater understanding of the littoral environment, the Office of Naval Research (ONR) has funded several, large, cooperative, research projects to study inlets in the U.S.. Specifically, in May-June, 2012 an experiment at the New River Inlet, known as the River and Inlet Dynamics experiment (RIVET) was conducted. RIVET 2 is currently scheduled for the Columbia River, in May, 2013. The New River Inlet is approximately 200 m wide with a very large back bay. While river is in the name of the inlet, there is no river forcing the inlet is actually tidally forced. The Columbia River is a different system in that it is approximately 2 km wide and has strong river forcing. A third system which is different from the systems described above is Elkhorn Slough which is a short (10 km), shallow (3 m), highly reflective system, where the tidal wave is a standing wave. From a short experiment conducted in the NPS field studies (OC4210) in 2009, differences were noticed in wave characteristics between the shoreward and seaward tidal wave. Due to a lack of statistical confidence in the measurements and the increased desire by the Navy to gain a better understanding of the physical environment of the littorals, a small field experiment was conducted to explore the tidal wave characteristics of a highly reflective estuary.

THIS PAGE INTENTIONALLY LEFT BLANK

II. INTRODUCTION

As a tidal wave propagates from the open ocean through the inlet and upstream into the estuary, it distorts due to changes in water depth, channel geometry and frictional effects (Friedrichs and Aubrey 1988; van Rijn 2010). The tidal distortion is generally represented by overtides (tidal harmonics of astronomical constituents) and compound tides (nonlinear sums and differences of all tidal constituents) that the astronomical tides develop in shallow water (Dronkers 1964; Uncles 1981; Speer and Aubrey 1985; Friedrichs and Aubrey 1988; Nidzieko 2010). The tidal wave distortion is described by the tidal asymmetry, which is the inequality of the ebb and flood tidal currents. The inequality determines the net sediment transport and flushing patterns (Dronkers, 1986; Friedrichs and Aubrey, 1988). For example, an ebb-dominated system is characterized by a shorter duration, fast ebb current relative to a longer duration, slower flood current, which is often associated with ebb-tidal delta morphologic feature (Boon and Byrne 1981).

Most of the original work on tidal asymmetry has focused on estuarine systems on the U.S. east coast, where the degree of the distortion is primarily described between the interaction of the M2, semidiurnal lunar tidal constituent, and the M4, the first overtide of M2 (Friedrichs and Aubrey 1988). Nidzieko (2010) expanding upon the work of Hoitink et al. (2003) and Woodworth (2005) demonstrated that the tidal asymmetry for mixed-mainly, semidiurnal, tidal regimes (i.e., short estuaries on the U.S. west coast) are produced primarily through the combination of the astronomical lunar (K1), lunisolar (O1) diurnal tides and M2. The phase relationship between K1, O1, and M2 induces an ebb-dominant tidal asymmetry because the lower-low water (LLW) follows the higher-high water (HHW) (Friedrichs 1995) and the phase of sea surface elevation and velocity are in quadrature (Nidzieko 2010). Though there is an ebb dominance at the estuary mouth, Nidzieko (2010) showed that the tidal asymmetry in short estuaries is modified as a function of distance upstream due to the increased amplitudes of the overtides and compound tides, consistent with the work by Friedrichs and Aubrey (1988). Nidzieko

(2010) provides examples of estuaries, where the upstream tidal asymmetry (distortion) becomes flood dominated, and others where the ebb dominance is enhanced.

An interesting question is raised about the behavior of the tidal distortion owing to the standing-wave nature of a short estuary. A standing-wave estuary implies that that shoreward propagating tidal wave is nearly perfectly reflected at the landward boundary. If the shoreward propagating wave becomes distorted as it travels landward, does this distortion decrease (or increase) as it reflected back toward the ocean? To examine the shoreward and seaward standing-wave structure of the tidal wave requires observations of both the potential (pressure) and kinetic (velocity) energy. However, most experiments tend to use pressure measurements solely, because pressure sensors are robust and inexpensive.

To address tidal evolution and distortion, a field experiment was performed in fall of 2011 in Elkhorn Slough (ES), CA, which is one of the short estuaries discussed by Nidzieko (2010). Owing to the standing-wave structure, an array of four co-located pressure and velocity sensors were deployed throughout the slough, such that shoreward and seaward tidal signal can be separated. The separated signals allow for an accurate description of the shoreward and seaward tidal propagation and corresponding distortion. To date, this is the first time that this approach is applied to tidal wave motions using field observations. The amount of tidal wave reflection for the astronomical constituents, overtides, and compound tides are described. The characteristics of the shoreward and seaward tidal wave distortion and the mechanisms responsible for the distortion are discussed.

III. EXPERIMENT SETUP AND DATA COLLECTION

ES is located at the center of Monterey Bay (MB) and is adjacent to the landward edge of the Monterey Submarine Canyon. The Monterey Bay Sea Floor Mapping Lab (MBSFML) at California State University Monterey Bay (CSUMB) performed high-resolution bathymetric surveys of ES between September-December, 2011 (Figure 1). ES consists of approximately a 12 km main channel that is 200 m wide near the mouth and narrows upstream to 90 m at Parson Slough (Broenkow and Breaker 2005). The length of ES is only 3.5% of the semi-diurnal tidal wavelength. The channel from the edge of the man-made jetties to the HW1 bridge is approximately 4.5 m deep. East of the HW1 bridge, there is an abrupt reduction in the water depth to 2.5 m (Figure 1). There is no channel dredging east of the bridge. There are a number of depth undulations along the channel, but the average slope is 1:4000. The deepest part of the channel is 10 m and is associated with erosion by secondary circulation around Seal Bend (Figure 1). ES is surrounded by extensive Salicornia marsh and mud flats with a number of small tributaries (Broenkow and Breaker 2005). At low tide, the slough is a narrow channel with a large area of exposed dry marsh and mud flats, while at high tide the marsh and mud flats are inundated.

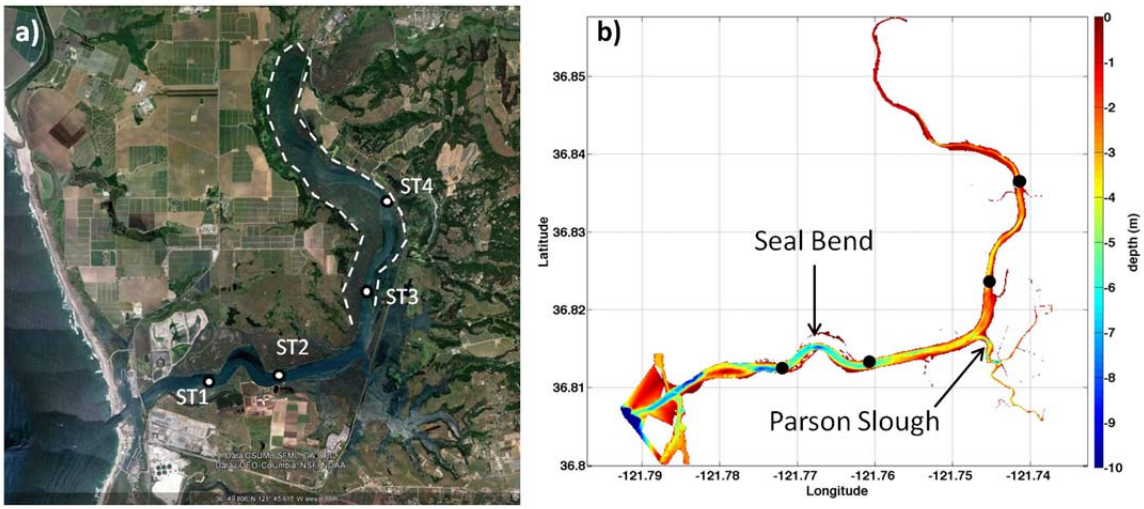

Figure 1. a) Google Earth image of Elkhorn Slough showing location of the 4 ADCP locations with white dots. The white dashed line highlights the low-lying marsh and mud flats at the shoreward end of the slough. b) 2011 bathymetry map of ES provided by CSUMB SFML. ADCP locations are shown with black dots. Depth color-scale provided on the right.

The slough is well-mixed, lacking stratification with water properties closely resembling MB (Broenkow and Breaker 2005). The dominant current direction in ES is streamwise flow, and secondary lateral circulations generated by curvature in the bends of the slough are expected to cause flows to depart from the streamwise orientation (Wong 1989; Broenkow and Breaker 2005; Breaker et al. 2008; Nidzieko et el. 2008). Research has found that the tidal elevation and velocity in ES of the diurnal and semidiurnal tidal wave are approximately in quadrature as the result of standing-wave characteristics (Wong 1989; Broenkow and Breaker 2005). The inefficient water exchange at high tide due to the extensive Salicornia marsh and mud flats and numerous small tributaries throughout ES are believed to enhance longer flood currents and shorter more intense ebb currents (Wong 1989; Broenkow and Breaker 2005). The wetting and drying of the marsh and mud flats are hypothesized as the mechanism for enhancing tidal asymmetry (Wong 1989; Broenkow and Breaker 2005; Nidzieko 2010).

Four 2-MHz Acoustic Doppler Current Profilers (ADCPs) with co-located pressure sensors were deployed longitudinally throughout ES channel for 66 days in Sept-Oct 2011 (Figure 1). The upward-oriented ADCPs were mounted on 1m-high Ocean

Science Group sea spider tripods. The four sensor locations were strategically placed throughout the slough. Station 1 and 2 (ST1, ST2) were located on opposing ends of Seal Bend 2.5 and 3.5 km from the mouth, respectively. Station 3 (ST3) was located upstream of the connection to Parson Slough 5.5 km from the mouth. Note that Parson Slough is an approximately 50 m wide opening that connects to a complex set of tidal tributaries and marsh (Broenkow and Breaker, 2005). Station 4 (ST4) was located farther upstream approximately 500 m from Kirby Park and 7 km from the mouth of ES. The reflection point in ES is located approximately 12 km from the mouth.

Velocities were obtained at 50 cm bin intervals sampled at 1Hz and averaged over 90s before being stored. Owing to the minimal vertical variation, horizontal velocities were depth-averaged and rotated to the streamwise orientation. The relative across-channel variability described as the ratio of the across-channel velocity standard deviation to the streamwise standard deviation is 8%, 13%, 7%, and 7 % for ST1–4. The flow at ST1, 3 and 4 is considered streamwise dominant, whereas ST2 has more variability its proximity to the secondary circulation associated with the large curvature by Seals Bend (Breaker et al. 2008; Nidzieko et al. 2008).

The ocean tide sea surface elevation for the corresponding ADCP deployment times was obtained from the NOAA tidal station (#9413450) located 23.5km south of the entrance to Moss Landing in 7.3 m of water. The station uses a pressure sensor sampling at 6 minutes.

THIS PAGE INTENTIONALLY LEFT BLANK

IV. METHODOLOGY

To describe the evolution and distortion of the shoreward (+) and the reflected seaward (-) propagating tidal wave, the sea surface elevation (η±) time series are constructed from collocated pressure head (p) and depth-averaged streamwise velocity (u) assuming shallow water,

$$\eta^{\pm} = 1/2\left[p \pm (u\sqrt{\frac{h}{g}}) \right] \quad (1)$$

where h is average water depth and g is the gravitational acceleration (Guza et al. 1984). This approach successfully described the cross-shore energy fluxes of infragravity waves in the nearshore surf zone environment (Guza et al. 1984; Elgar and Guza 1985; List 1992; Sheremet et al. 2002). Tidal constituent amplitudes (A) and phases (θ) for astronomical, overtides, and compound tides are computed for the p, and η± time series using the T_TIDE harmonic analysis program (Pawlowicz et al. 2002). For a 66-day time series record, T_TIDE analysis resolves 35 tidal constituents describing 98% of the signal, where 2% of the signal is considered non-tidal residual motion. Only p and u are used to separate the signal, the across-channel velocity (v) is not considered. Large variability in the across-channel velocity (v) can bias η± estimates. Owing to the large v at ST2 and potential to bias η± estimates, results for ST2 will be omitted unless the variable of interest is p.

In an effort to parameterize the tidal evolution and distortion, the tidal amplitudes are summed over two different frequency (f) bands, where the frequency cut-off between the frequency bands is 0.1 cycles per hour (cph). T_TIDE amplitudes are summed for f<0.1 cph, which represent the primary astronomical forcing (i.e., M2, K1, O1, among others), referred to as low-frequency motions (subscript lfm). Amplitudes summed for f>0.1 cph represent tidal harmonics, such overtides (e.g., M4, among others), that are primarily used to characterize the tidal distortion, and are referred to as high-frequency motions (subscript hfm). Note that the total (subscript tot) respresents the combined sum of both the low- and high-frequency motions. Summed tidal amplitudes for the low-

frequency, high-frequency, and total motions are estimated for p and η± (discussed below) and will be dennoted with subscripts.

Tidal amplitude reflection (R) is the ratio of the square root of the seaward energy flux divided by the shoreward energy flux,

$$R = \sqrt{\frac{\frac{1}{2}\rho g\left(A^{-}\right)^{2} C_g b}{\frac{1}{2}\rho g\left(A^{+}\right)^{2} C_g b}} = \sqrt{\frac{\left(A^{-}\right)^{2}}{\left(A^{-}\right)^{2}}} \qquad (2)$$

where ρ is the density of sea water, C_g is the shallow water wave group speed, and b is the channel width (Sheremet et al. 2002). When R=1, the tidal wave is perfectly reflected in the estuary and there are no energy losses in the system. An R<1 implies that there is tidal wave energy losses and R>1 implies there is an additional source of energy. Low-frequency, high-frequency, total R are computed for ST1, 3, and 4 (Table 1).

	ST1	ST3	ST4
R_{tot}	95	102	100
R_{lfm}	90	94	92
R_{hfm}	125	224	231

Table 1. Reflectivity coefficients for the total, lfm and hfm for ST1, ST3 and ST4.

V. RESULTS

The behavior of the tidal wave is described by tidal constituent amplitude spectra for measured pressure signals at MB and ST4 in ES (Figure 2). Low-frequency spectral amplitudes associated with the astronomical tidal forcing represent most of the tidal variance and are similar at both stations. The high-frequency spectral amplitudes are zero at MB, but increase farther upstream in ES. The high-frequency spectral amplitudes are integer multiple harmonics (i.e., M4, M6) of the astronomical forcing (i.e., K1, O1, M2) (Figure 2). The amplitude spectra are consistent with previous spectra measured ES by Broenkow and Breaker (2005) and Nidzieko (2010).

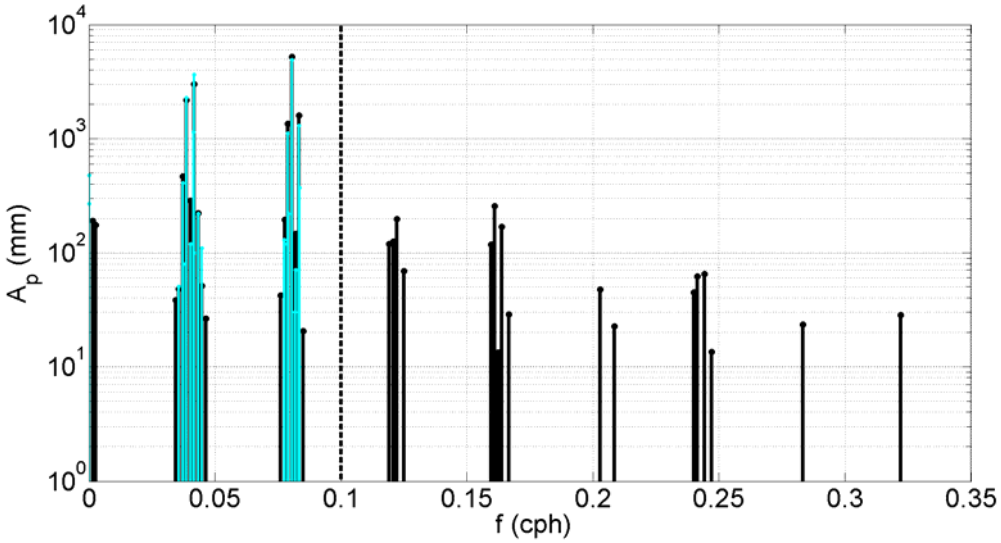

Figure 2. Tidal constituent amplitudes estimated T_TIDE at ST4 in ES from pressure (black lines) and the long-term NOAA tidal constituents at the MB station. Vertical black dashed line at f=0.1 cph represents the frequency cut-off that separates the low-frequency motions to the left and the high-frequency motions to the right.

There is a 16% increase in A_{tot} from MB to ST4 in ES (Figure 3a) estimated by linear regression. This trend can be explained by the analytical solution for a co-oscillating tide. Lamb (1932) provides solutions for various simple geometric inlet

configurations. Of the configurations, ES is best described as constant width (b), linear varying water depth (h) resulting in a solution defined as,

$$\eta = c\frac{J_o\left(2\sqrt{kx}\right)}{J_o\left(2\sqrt{kl}\right)}\cos(\sigma t + \varepsilon) \tag{4}$$

where J_o represents the zero-order, first-kind Bessel function, $k = \sigma^2 l / gh_o$, l is the slough length, h_o is the slough depth at the end of the channel, σ is the radian tidal frequency, x is distance from the landward boundary, C is the tidal amplitude, ε is the phase difference. Equation 3 applied to ES geometries results in an 11% increase in amplitude from the mouth to the head of the slough, consistent with the measurements (Figure 3a). While there is a difference between the model and measurements, the model describes the general co-oscillating tidal wave characteristic well considering the over simplification of the slough (constant width).

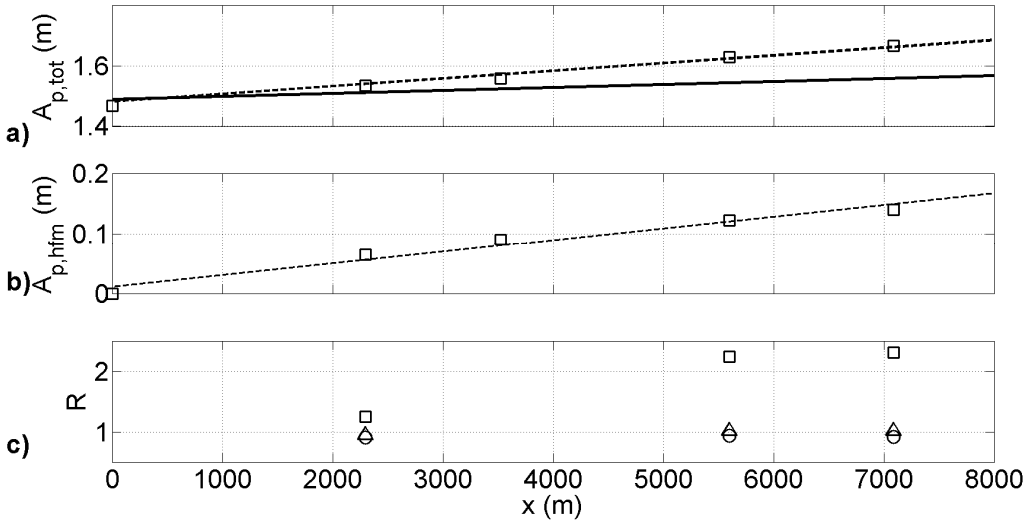

Figure 3. a) Squares represent A_{tot} between MB and ST4 as a function of along-channel distance. The dashed line is the best-fit line for A_{tot} estimated by linear regression. Solid line represents the Lamb (1932) analytical solution for co-oscillating tide for ES. b) $A_{p,hfm}$ (squares) between MB and ST4 as a function of along-channel distance. The dashed line is the best-fit line for $A_{p,hfm}$ estimated by linear regression. c) R_{tot} (triangles), R_{lfm} (circles), and R_{hfm} (squares) as a function of along-channel distance.

The $A_{p,hfm}$ (estimated with pressure) steadily increases from 0 to approximately 14 cm between MB and ST4 (Figure 3b). The increase in the tidal wave non-linearity with along-channel distance associated with pressure signal is consistent with previous research (Speer and Aubrey 1985; among others). However, the measured pressure signal represents the potential energy portion of a tidal wave. A purely progressive wave can be described solely by pressure or velocity because they are in phase. For a standing-wave, both potential and kinetic energy must be considered to effectively characterize the wave (i.e., Equation 1).

The reflection coefficients, R (Equation 2), for each station for the total, low-frequency, and high-frequency related shoreward and seaward tidal signal provide insights to the bulk tidal wave characteristics and its evolution. The R_{tot} ranges from 95%–102% (Figure 3c, Table 1). The small differences in R_{tot} are related to the fact that the propagating shoreward and seaward tidal can behave different at the different stations. Owing to this, ST1 represents the overall tidal behavior in the slough, because it is located the farthest from the upstream boundary and describes the reflection over a longer distance, whereas ST3–4 represents the tidal behavior farther upstream. The R_{tot} results imply that farther upstream the tide is more reflected than downstream. For ST1, 5% of the total amplitude is dissipated presumably by bottom friction (Speer and Aubrey 1985) or secondary circulation associated with Seal Bend (Broenkow and Breaker 2005; Breaker et al. 2008; Nidzieko et al. 2008). In addition, the marsh and mud flats of Parson Slough located between ST1 and ST3 may contribute to the reflection at ST1 and its difference measured at ST3–4. ST3 and ST4 are closer to the reflection point and the complexities of the slough are much less, as there are minimal tidal tributaries and mostly marsh and mud flats. The high R_{tot} at each station suggest ES is highly reflective, consistent with Broenkow and Breaker (2005), Breaker et al. (2008) and Nidzieko (2010).

R_{lfm} at ST1, 3 and 4 are 90%, 94% and 92%, while R_{hfm} at ST1, 3 and 4 are 125%, 224% and 231%, respectively (Figure 3c, Table 1). R_{lfm} indicate approximately 10% energy loss compared to the gain in energy associated with R_{hfm}. Owing to the fact that R_{tot} represents contributions from R_{lfm} and $R_{hfm,}$ and that R_{tot} is ~100%, then the $A_{\eta+,hfm}$ of

the seaward wave must be more non-linear than the $A_{\eta-,hfm}$ of the shoreward wave. The larger $A_{\eta+,hfm}$ of the seaward wave results in a R_{hfm} greater than 100% and accounts for the 10% energy loss associated with R_{lfm}. The larger R_{hfm} value suggests energy is actually transferred from the low-frequency tidal motions (i.e., astronomical constituents) to the high-frequency tidal motions (i.e., harmonics) (Parker 1991). These are new findings previously unavailable from only pressure measurements.

VI. DISCUSSION

The previous section highlighted the differences between the shoreward and seaward waves using bulk statistics, but the bulk statistics do not describe and explain why the waves are actually different. Many researchers believe that tidal distortion in estuaries with a main channel and vast low lying marsh and mud flats is due to inefficient water exchange around high tide as the marsh and mud flats become inundated (Nummedal and Humphries 1978; Boon and Byrne 1981; Speer and Aubrey 1985; Friedrichs and Aubrey 1988 Wong 1989; Broenkow and Breaker 2005; Breaker et al. 2008; Nidzieko 2010). Unfortunately, field measurements in this experiment were not obtained at the landward boundary to describe the effects of the marsh, but the time signals of the shoreward and seaward tidal wave are available to provide insight on the behavior that occurs at the landward boundary, which is examined next.

The characteristics of a measured 24-hr time signal for yearday 269 of the shoreward (Figure 4, solid lines) and seaward (Figure 4, dashed lines) tidal wave for ST1, ST3 and ST4 are evaluated. The shoreward tidal wave first propagates by ST1 (Figure 4, blue line) and then to ST3 (Figure 4, green line) and onto ST4 (Figure 4, red line), which is shown by the temporal offset between the stations. The temporal lag between each station represents the propagation time that is dependent upon the distance between the stations (e.g., the largest distance is between ST1 and ST4 resulting in the largest temporal difference). The seaward time signals (Figure 4, solid lines) are similar to shoreward time signals (Figure 4, dashed lines), except in reverse. The seaward time signal represents the tidal wave that has propagated to the landward boundary and reflected downstream. Therefore, ST4 represents the first station that the tidal seaward wave encounters, and then the tidal wave propagates past ST3 and then ST1. The time difference between the shoreward signal and the seaward signal represents the time the tidal takes to propagate to the landward boundary and back, which is referred to as the reflection time. The reflection time increases with increasing distance downstream from the landward boundary. The reflection time is largest for ST1.

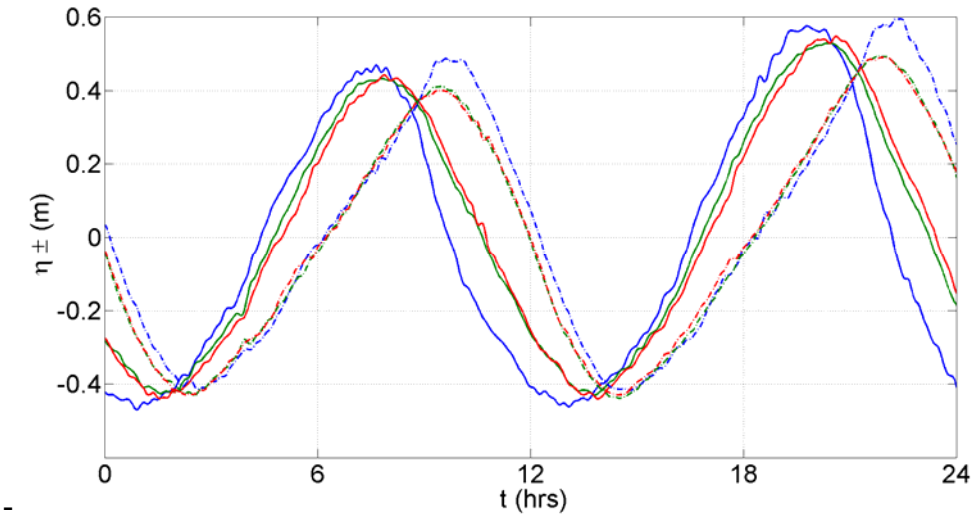

Figure 4. The shoreward (solid lines) and seaward (dashed lines) sea surface elevation measured for yearday 269 (shown in relative hours) for ST1 (blue), ST3 (green), and ST4 (red).

The time difference between the shoreward and seaward time signal steadily increases (Figure 4) from low tide to high tide implying that the reflection time is changing and appears to be a function of elevation (total depth). The reflection time decreases from high tide to low tide and the response differs slightly from station to station (Figure 4). The reflection time for high tide maxima and low tide minima are estimated for the 66-day record for ST1, ST3, and ST4, resulting in four estimates per day. A linear trend is found between the reflection time and the sea surface elevation, which increases with increasing elevation (Figure 5). The linear slopes are 0.83, 0.99, and 0.87 for ST1, ST3, and ST4 suggesting about a 1 hr time lag per meter of elevation gain. Though a linear trend is observed, there is a variability indicated by r^2-values of 0.59, 0.69, and 0.60 for ST1, ST3, and ST4. The large scatter at ST1 (Figure 5a) may be related to influence of Parson Slough or Seal Bend. ST3 and ST4 interestingly have reduced variability at low tide (Figure 5b,c) suggesting that the reflection time below MSL is controlled by the channel and above MSL controlled by the more complex nature of the mud flats and marshes.

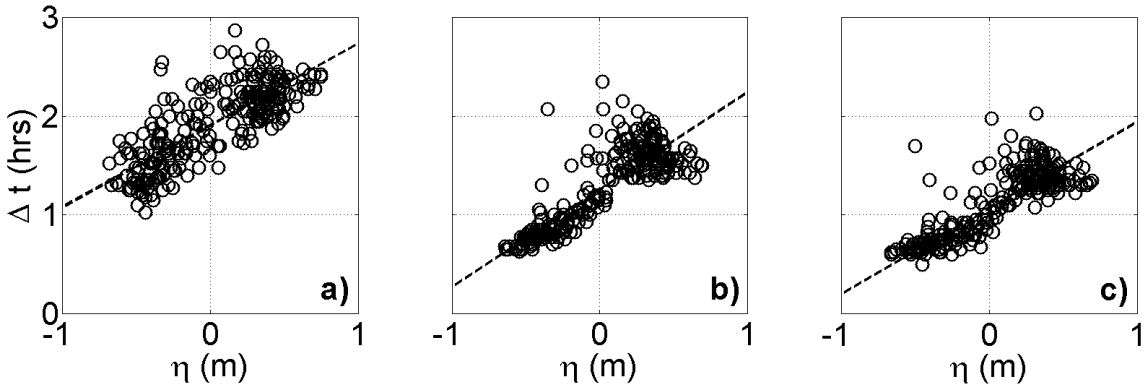

Figure 5. The reflective time lag estimated from daily high tide and low tide maxima and minima for a) ST1, b) ST3, and c) ST4. Dashed line represents the best-fit line estimated with linear regression. The linear slopes are 0.83, 0.99, and 0.87 and the r^2-values are 0.59, 0.69, and 0.60 for ST1, ST3, and ST4.

These results are initially counter-intuitive, because it is expected as the depth of the main channel increases (decreases) with a rising (falling) tide, the phase speed, $\sqrt{g(h+\eta)}$, of the tidal wave would increase (decrease) [Friedrichs and Aubrey 1988; Wong 1989; Broenkow and Breaker 2005] and decrease the reflection time which differs with the observations. The total water depth (h+η) assumes that the channel has vertical walls. While this is relatively true for some portions of the slough located downstream, at the upper end of the slough the channel is surrounded by shallow marsh and mud flats (Figure 1), which becomes inundated at higher tides (Broenkow and Breaker 2005). Since the channel cannot be described by simple rectangle, the average (effective) water depth is estimated by

$$h_{avg} = A_c / b \quad , \tag{5}$$

where A_c is the cross-sectional area and b is the channel width. Therefore, increasing tidal elevation results in a decrease in average water depth as water spreads out over the marsh. The result is a decrease in phase speed and increased reflection time as observed (Figures 4 and 5). This is consistent with the results found for a progressive wave system by Friedrichs and Aubrey (1988), where the volume of intertidal storage divided by the

channel volume is large in relation to the tidal amplitude divided by water depth that caused the wave at high tide to propagate slower than at low tide.

The difference in reflection time as function of elevation modifies the seaward tidal signal relative to the shoreward time signal, which explains why the seaward tidal wave becomes more distorted. If the reflection time is constant, then the shoreward and seaward waves would be the same. However, this cannot happen even in a rectangular channel because the phase speed would increase with increasing depth (Friedrichs and Aubrey 1988). This suggests that the seaward tidal wave will always be more distorted than the shoreward tidal wave in a reflective estuary.

VII. SUMMARY AND CONCLUSIONS

Co-located measurements of pressure and depth-averaged velocity measured longitudinally throughout a short slough, allowed the tidal signal to be separated into shoreward and seaward tidal signals, providing new insights into tidal wave characteristics. The overall tidal wave reflection in Elkhorn Slough, CA, is high (~100%). The low-frequency seaward tidal signal, associated with astronomical tidal constituents, tends to lose 10% of its amplitude relatively to the shoreward tidal signal, whereas, the high-frequency seaward tidal signal, associated with tidal harmonics, has a large (>125%) increase in amplitude relative to the shoreward tidal signal. The increase in amplitude of the high frequency seaward tidal signal suggests energy is transferred from the astronomical tidal constituents to the harmonics and overtides consistent with the findings of Parker (1991). The high-frequency amplitudes are responsible for the tidal wave distortion resulting in the seaward tidal wave being more distorted than the shoreward tidal wave. The mechanism responsible for the seaward tidal wave distortion can be explained by the shallow-water wave phase speed, which is depth dependent. As the tidal elevation increases, the small channel near the landward boundary fills up quickly and water flows onto the adjacent shallow mud flats and marshes reducing the effective depth of the channel. The decreases in the effective depth reduces the shallow-water wave phase speed inducing a reflective time lag, defined as the time the tidal wave takes to propagate upstream to the landward boundary and back. A near linear trend was found for the reflective time lag that increases with increasing elevation for all stations. This trend effectively modifies the characteristic of the seaward tidal signal relative to the shoreward tidal signal, which causes the tidal wave distortion. In summary, the reflective behavior of the slough is responsible for the increase in tidal distortion for the seaward tidal wave.

THIS PAGE INTENTIONALLY LEFT BLANK

LIST OF REFERENCES

Aubrey, D. G. and P. E. Speer, 1985: A study of non-linear tidal propagation in shallow inlet estuarine systems. Part 2. Theory, *Estuarine Coastal Shelf Sci.,* **21,** 207–224.

Boon, J. D., and R. J. Byrne, 1981: On basin hypsometry and the morphodynamic response of coastal inlet systems. *Marine Geology,* **40,** 27–48.

Breaker, L. C., W. W. Broenkow, W. E. Watson, and Y. H. Jo, 2007: Tidal and nontidal oscillations in Elkhorn Slough, California. *Estuaries and Coasts.,* **31,** 239–257.

Broenkow, W. W., and L. C. Breaker, 2005. A 30-year history of tide and current measurements in Elkhorn Slough, California (November 18, 2005). *Scripps Institution of Oceanography Library.* Paper 8. http://repositories.cdlib.org/sio/lib/8.

Dronkers, J. J. 1964: *Tidal computations in rivers and coastal waters*. North-Holland Pub. Company, 518 pp.

Dronkers, J. (1986), Tidal asymmetry and estuarine morphology, *Neth. J. Sea. Res.,* **20,** 117–131.

Elgar, S., and R. T. Guza, 1985: Observations of bispectra of shoaling surface gravity waves, *J. Fluid Mech.,* **161,** 425–448.

Friedrichs, C. T., 1995: Stability shear stress and equilibrium cross-sectional geometry of sheltered tidal channels. *J. Coastal Res.,* **11,** 1062–1074.

Friedrichs, C. T., and D. G. Aubrey, 1988: Non-linear distortion in shallow well-mixed estuaries: A synthesis. *Estuarine, Coastal and Shelf Sci.,* **27,** 521–545.

Friedrichs, C. T., and D. G. Aubrey, 1994: Tidal propagation in strongly convergent channels, *J. Geophys. Res.,* **99,** 3321–3336.

Guza, R.T., E.B. Thornton, and R.A. Holman, Swash on steep and shallow beaches, paper presented at 19th Coastal Engineering Conference, Am. Soc. Of Civ. Eng., Houston, Tex., 1984

Hoitink, A. J. F., P. Hoekstra, and D.S. van Maren, 2003: Flow asymmetry with astronomical tides: Implications for the residual transport sediment, *J. Geophys. Res.,* **108,** C103315, doi:10.1029/2002JC001539.

Lamb, H., 1932: *Hydrodynamics.* 6th ed. Dover Publications, 738 pp.

List, J. H., 1992: A model for the generation of two-dimensional surf beat, *J. Geophys. Res.,* **97,** 5623–5635.

Nidzieko, N. J., Hench, J. L., and Monismith, S. G., 2009: Lateral circulation in well-mixed and stratified estuarine flows with curvature, *J. Phys Oceanogr.,* **39,** 831–851.

Nidzieko, N. J., 2010: Tidal asymmetry in estuaries with mixed semidiurnal/diurnal tides, *J. Geophys. Res*., **115,** C08006, doi:10.1029/2009JC005864.

Nummedal, D. and Humphries, S. M., 1978: Hydraulics and dynamics of the North Inlet, 1975–1976, *G.I.T.I. Report 16, U.S. Army Coastal Engr. Res. Cent.,* 214 pp.

Parker, B. B., 1991: The relative importance of the various nonlinear mechanisms in a wide range of tidal interactions, In *Tidal Hydrodynamics,* B. B. Parker, Ed., John Wiley & Sons, 237–268.

Pawlowicz, R., B., Beardsley, and S, Lentz,2002: Classical tidal harmonic analysis including error estimates in MATLAB using T-TIDE. *Computers & Geosciences,* **28(8)**, 929–937. doi:10.1016/S0098–3004(02)00013–4

Sheremet, A., R.T. Guza, S. Elgar, and T.H.C. Herbers, 2002: Observations of nearshore infragravity waves: Seaward and shoreward propagating components, *J. Geophys. Res.,* **107,** C83095, doi:10.1029/2001JC000970.

Uncles, R. J., 1981: A note on tidal asymmetry in the Severn Estuary, *Estuarine Coastal Shelf Sci.,* **13,** 419–432.

van Rijn, L. C., 2010: Tidal phenomena in the Scheldt Estuary, *Deltares*: Delft. I, 99 pp.

Woodworth, P. L., Blackman, D. L., Pugh, D. T., and Vassie, J. M., 2005: On the role of diurnal tides in contributing to asymmetries in tidal probability distribution functions in areas of predominantly semi-diurnal tide, *Estuarine Coastal Shelf Sci.,* **64,** 235–240.

Wong, C.S. 1989: Observations of tides and tidal currents in Elkhorn Slough, California. M.S. thesis, Moss Landing Marine Laboratories, San Jose State Unniversity, 93 pp.

INITIAL DISTRIBUTION LIST

1. Defense Technical Information Center
   Ft. Belvoir, Virginia

2. Dudley Knox Library
   Naval Postgraduate School
   Monterey, California